

Supporting Information

Pressure-induced Emission Enhancement by Restricting Chemical Bond Vibration

Zhiyuan Fu,^{a,‡} Haichao Liu,^{b,‡} Jingyi Zhao,^c Xiangyu Zhang,^b Xiaoyan Zheng,^{c,*} Bing Yang,^{b,*} Xinyi Yang,^a Kai Wang,^{a,*} Bo Zou^a

^aState Key Laboratory of Superhard Materials, College of Physics, Jilin University, Changchun 130012, P. R. China

^bState Key Laboratory of Supramolecular Structure and Materials, College of Chemistry, Jilin University, Changchun 130012, P. R. China

^cBeijing Key Laboratory of Photoelectronic/Electrophotonic Conversion Materials, Key Laboratory of Cluster Science of Ministry of Education, School of Chemistry and Chemical Engineering, Beijing Institute of Technology, Beijing 100081, P. R. China.

KEYWORDS: high pressure, pressure-induced emission enhancement (PIEE), hydrogen bonds, the restriction of chemical bonds vibration, aggregation-induced emission enhancement (AIEE).

Contents

SI Experimental Methods	S3
Sample Preparation and High-Pressure Generation	S3
Optical Measurements	S3
ADXRD Measurements	S3
Computation Details	S3
SII Figures and tables	S4
Figure S1. Molecular structure and packing arrangement of DBTS	S4
Figure S2. AIE characteristic	S5
Figure S3. NTOs of DBTS monomer and dimer.....	S6
Table S1. Absorption and emission properties of DBTS	S7
Figure S4. Excitation spectra of DBTS crystal.	S7
Figure S5. Plot of emission wavelength and intensity against pressure.....	S8
Figure S6. Calculated π - π distance of DBTS on different pressure	S8
Figure S7. The calculation details of relaxation energy	S9
Table S2. Relaxation energy calculations.....	S10
Table S3. Vibrational normal modes of DBTS	S11
Table S4. The C \cdots C interactions on Hirshfeld surface	S13
Figure S8. Contribution rate of C \cdots C interactions to the Hirshfeld surface	S14
SIII Reference	S15

SI Experimental Methods

Sample Preparation and High-Pressure Generation: Dibenzothiothiophene 5,5-dioxide was purchased from TCI (Dibenzothiothiophene Sulfone, D4153) and used directly without purification. The high-pressure experiments were performed by the DAC. The sample was placed in the T301 gasket hole with a diameter of 150 μm and a thickness of 40 μm . And a small ruby ball was placed next to the sample for in-situ pressure calibration. In the high-pressure PL and ADXRD experiments, silicone oil (Aldrich) was used as the pressure-transition medium (PTM). KBr was used as the PTM in IR experiments.

Optical Measurements: In-situ high-pressure PL and absorption photos of the samples were shot by Canon Eos 5D mark II equipped with Nikon Eclipse TI-U microscope. The absorption spectra light source adopted deuterium-halogen light source, and the PL excitation source was the 355 nm line of a UV DPSS laser. The Spectrometer adopted Ocean Optics QE65000 spectrometer. IR micro spectroscopy of DBTS was carried out on Nicolet iN10 microscope spectrometer (Thermo Fisher Scientific, USA) using a liquid-nitrogen-cooled detector. The excitation spectra and AIEE experiments measurements were carried out on Edinburgh FLS980.

ADXRD Measurements: In situ high-pressure powder ADXRD experiments were carried out with the support of 4W2 beamline at Beijing Synchrotron Radiation Facility with a wavelength of 0.6199 \AA . The ADXRD patterns were collected for 300 s at each pressure and then were integrated with FIT2D program. The lattice parameters were analyzed by Materials Studio using ADXRD data.

Computation Details: Geometry optimization was performed for the DBTS at different pressures, based on the first principles plane-wave pseudopotential density functional theory^[1] as implemented in the CASTEP package.^[2] The starting structure DBTHPS02 (Deposition Number 1051696) was obtained from the Cambridge Structure Database. The functional GGA and PBE was used in the calculation.^[3] Using TS method for DFT-D correction.^[4] The convergence levels for total energy, max force, max stress, max displacement, and SCF iterations were fine. Hirshfeld surfaces and contributions of intermolecular contacts to the Hirshfeld surface area were calculated by Crystal Explorer 17.5.^[5-7] We also could get information about relative contributions of intermolecular contacts to the Hirshfeld surface area from it. The equilibrium structure of the molecule in the S_0 and S_1 states was obtained at the density functional theory (DFT) / time-dependent DFT (TD-DFT) level, respectively. All the DFT/TD-DFT calculations were carried out using Gaussian 09 (version D.01) package on a PowerLeader cluster.^[8] The frequency analysis of DBTS monomer was performed at the B3LYP/6-31G (d, p) level. The relaxation energy was analyzed by using DUSHIN program developed by Reimers.^[9] The absorption and emission properties of DBTS monomer and DBTS dimer, including wavelengths and natural transition orbitals (NTOs), were obtained at the B3LYP-GD3/6-31G (d, p) level. At high pressure, the molecular equilibrium geometry of S_0 and S_1 and the frequency of the regular mode were obtained by using TPSSh functional and 6-31G** basis set. reorganization energy was calculated by MOMAP program.^[10-12]

SII Figures and tables

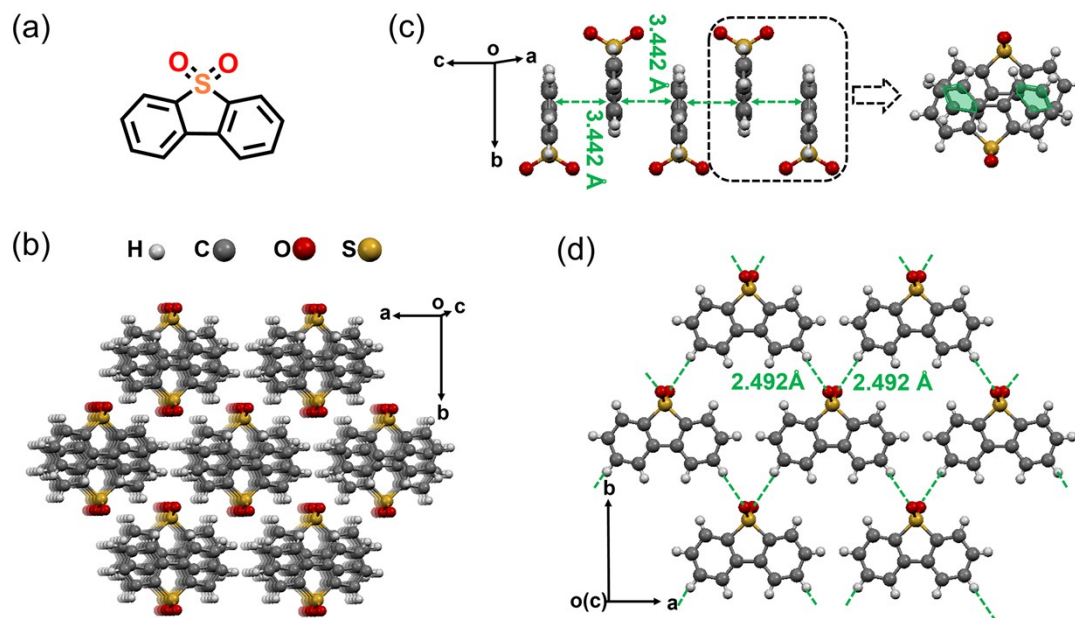


Figure S1. (a) Molecular structure of DBTS (b, c, d) Packing arrangement of DBTS crystal along different axes at ambient conditions.

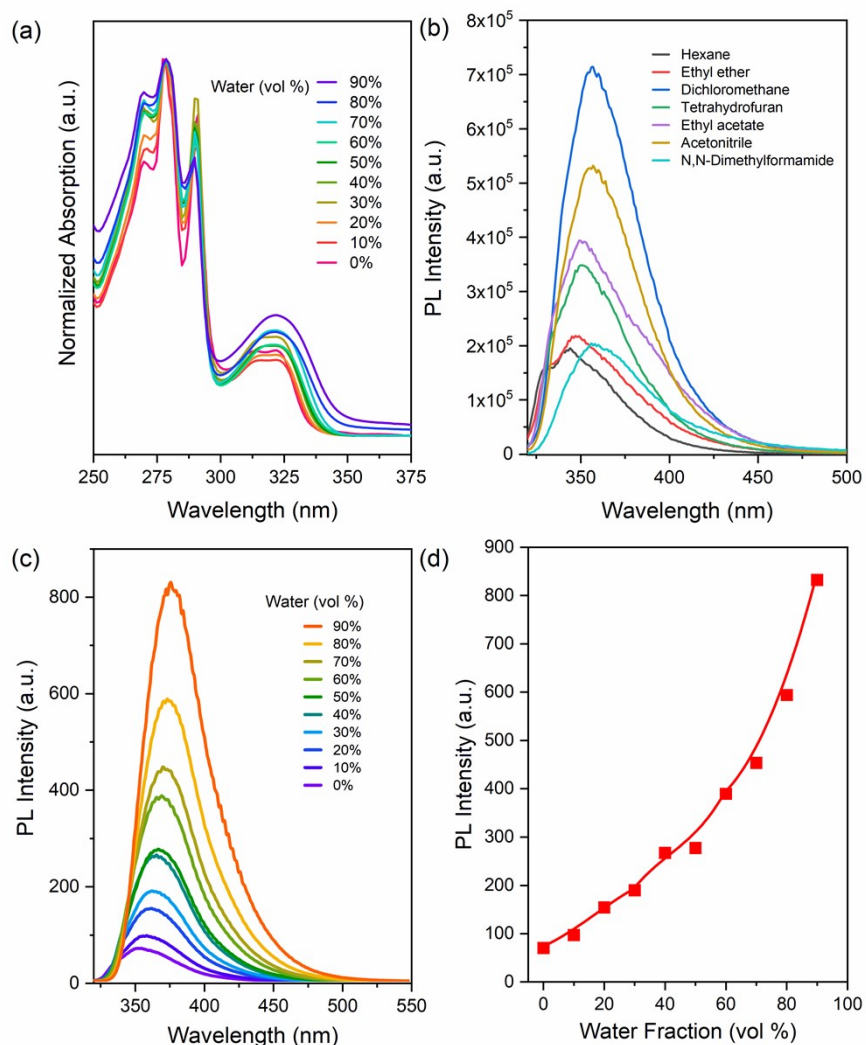


Figure S2. (a) Absorption spectra of DBTS in the THF-H₂O mixed solvent medium at different water fraction. (b) PL spectra of DBTS in different polar solvents. (c) PL spectra of DBTS (40 μM) in the THF-H₂O mixed solvent medium at different water fractions. ($\lambda_{\text{ex}} = 300 \text{ nm}$). (d) PL intensity with different water fraction.

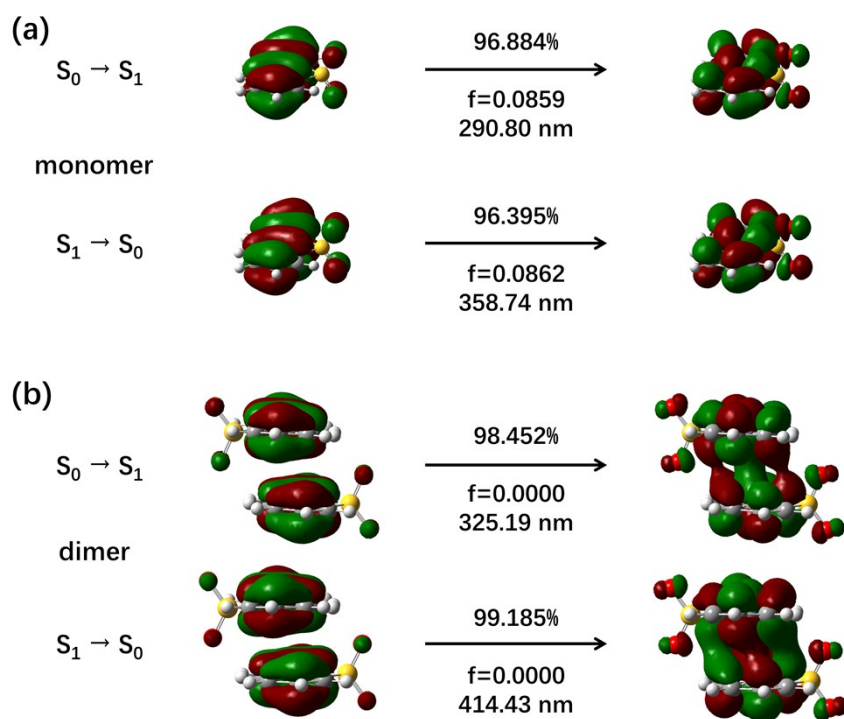


Figure S3. NTOs for $S_0 \rightarrow S_1$ and $S_1 \rightarrow S_0$ of (a) DBTS monomer and (b) DBTS dimer. NTOs were calculated based on the optimized ground state geometry for $S_0 \rightarrow S_1$ and the optimized excited state geometry for $S_1 \rightarrow S_0$, respectively.

As shown in **Figure S3**, relative to the NTOs of DBTS monomer, the NTOs of DBTS dimer show a large overlap of electron wavefunction between two DBTS monomers, which demonstrates a strong π - π interaction between two DBTS monomers. This large overlap of electron wavefunction explains the emission red shift of DBTS crystal relative to DBTS monomer in solution.

Table S1. Absorption and emission properties of DBTS in vacuum gas phase by TDDFT-B3LYP-GD3/6-31G (d, p) at the optimized geometries.

Molecules	Abs/Emi	Electronic transition	λ_{cal} (nm)	λ_{exp} (nm)
DBTS	Abs	$S_0 \rightarrow S_1$	290.80	323 (in Hexane)
	Emi	$S_1 \rightarrow S_0$	358.74	330, 344 (in Hexane)
DBTS dimer	Abs	$S_0 \rightarrow S_1$	325.19	355 (in crystal)
	Emi	$S_1 \rightarrow S_0$	414.43	405 (in crystal)

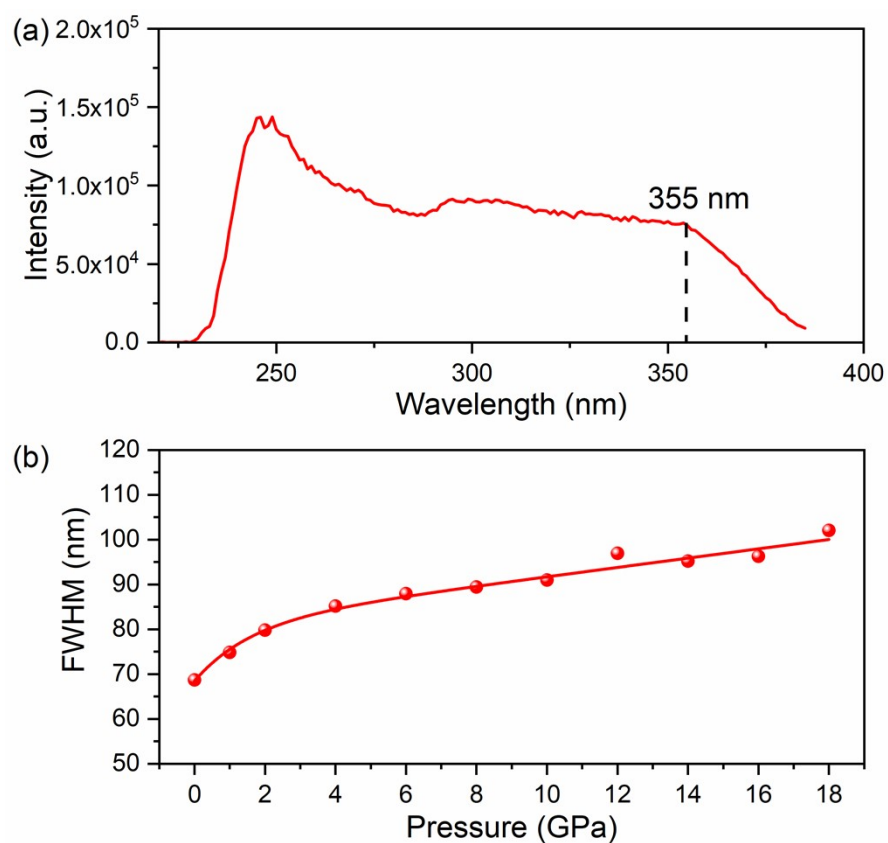


Figure S4. (a) Excitation spectra of DBTS crystal. (b) FWHM of DBTS gradually widened under pressure.

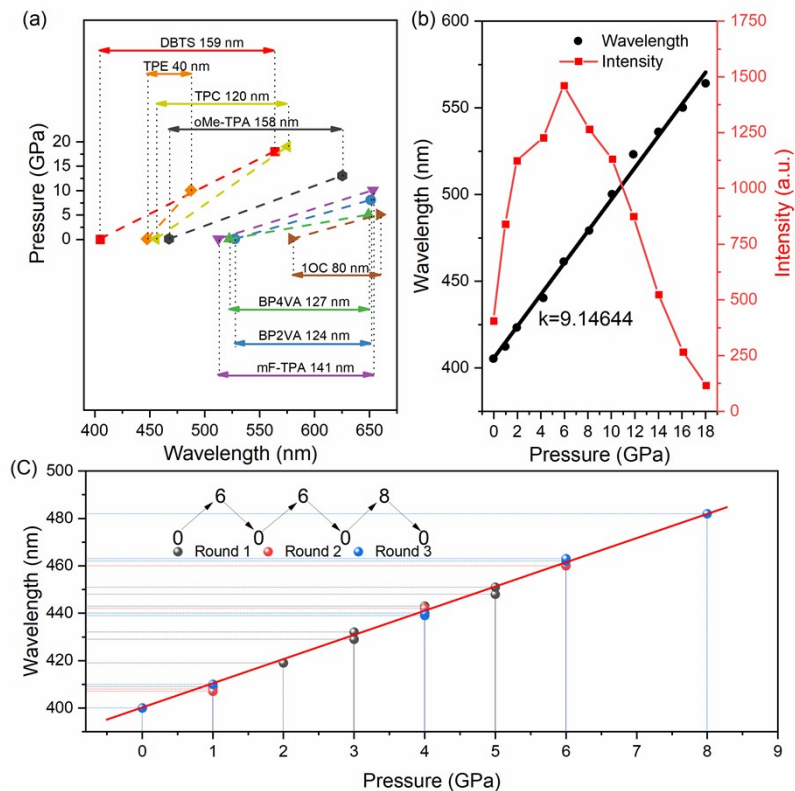


Figure S5. (a) The emission red shift of DBTS under pressure compared with other representative piezochromic materials. [13-19] (b) The PL wavelength and PL intensity under different pressure. (c) The DBTS was repeatedly pressurized to 6 GPa by DAC and then relieved, and finally pressurized to 8 GPa and then relieved, showed favorable recoverability.

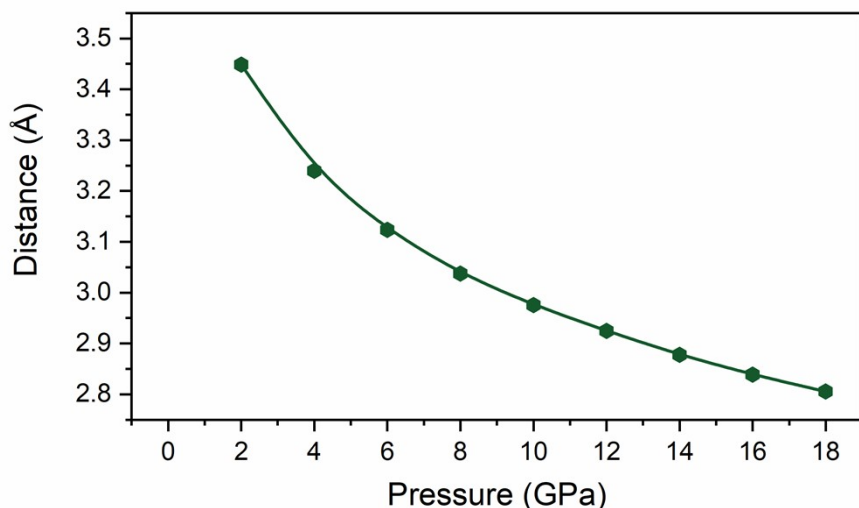


Figure S6. Calculated intermolecular π - π distance of DBTS on **different** pressure.

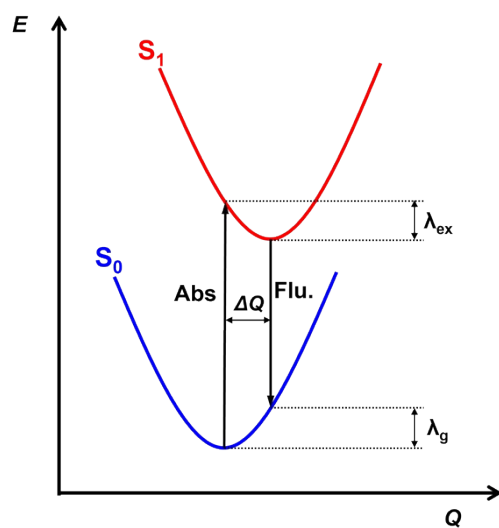
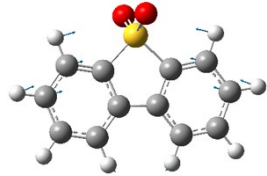
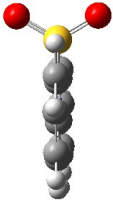
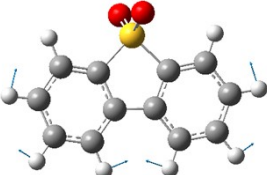
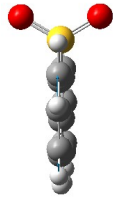
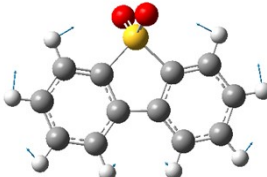
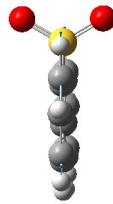
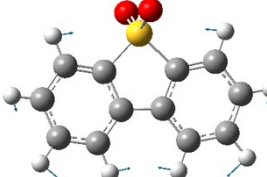
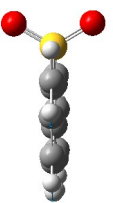
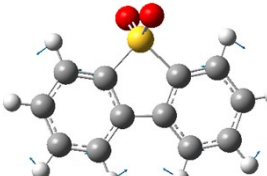
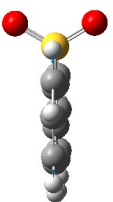
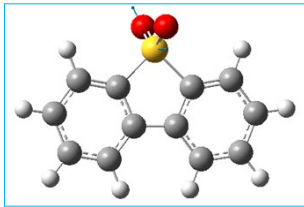
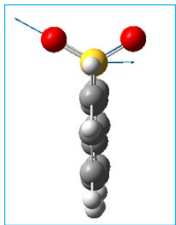


Figure S7. The calculation details of relaxation energy using the four-points approach. Here, the relaxation energies λ_g and λ_{ex} are along the potential energy surfaces of ground state (S_0) and excited state (S_1), respectively; the vertical axis is the energy E , and the horizontal axis is the normal mode displacement Q .

Table S2. The vibrational relaxation energy of DBTS along the ground state and excited state potential energy surface by DUSHIN.

Frequency (cm ⁻¹)	λ_g λ_i (cm ⁻¹)	Frequency (cm ⁻¹)	λ_{ex} λ_i (cm ⁻¹)
76	0	33	0
105	0	100	0
114	0	115	0
167	0.1	136	0
194	3.7	192	3.9
237	0	224	0
303	0	267	0
337	0	271	0
353	182.6	356	287.7
401	381.4	390	0
430	0	404	271.4
457	0	431	0
480	0	438	0
549	0	471	0
554	9.5	494	0
565	0	527	14.1
571	0	555	0
630	0	610	0
707	20.2	645	0
725	0	679	38.6
733	0	681	0
743	0	693	0
770	0	733	0
774	104	764	105.1
789	0	766	0
883	0	830	0
883	0	842	0
952	0	947	0
952	0	948	0
994	0	967	0
996	0	969	0
1021	0	979	0
1053	113.9	1007	8.4
1053	0	1009	0
1060	7.3	1016	1.7
1095	0	1048	0
1130	43.7	1093	321
1156	609.6	1152	638.8
1159	0	1167	0
1190	0	1171	0
1193	139.3	1186	27.7
1253	180	1190	0
1301	0	1224	12.4
1306	0	1280	0
1325	120.1	1363	0
1348	0	1368	58.2
1386	138.7	1395	96.6
1474	372.6	1462	0
1488	0	1471	161
1510	0	1488	0
1519	541.5	1515	0
1628	173	1539	534
1641	0	1555	175.4
1647	291.7	1602	0
1652	0	1605	494.3
3190	0	3193	0
3191	0.1	3195	0.1
3200	0	3200	0
3203	0	3202	0
3209	0	3213	0
3210	0.4	3213	0.1
3218	0	3220	0
3219	0.6	3221	0.9
$\lambda_g = 3434.0 \text{ cm}^{-1}$		$\lambda_{ex} = 3251.4 \text{ cm}^{-1}$	

Table S3. Vibrational normal modes of DBTS at ground state and excited state.

Molecules	Frequency (cm ⁻¹)	Front view	Side view
DBTS at ground state	401		
	1156		
	1474		
	1519		
	1647		
	1301 (S=O)		

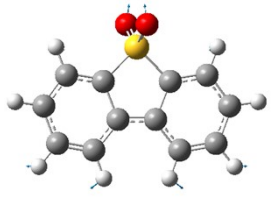
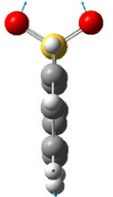
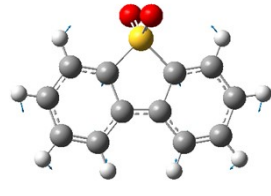
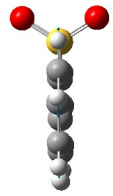
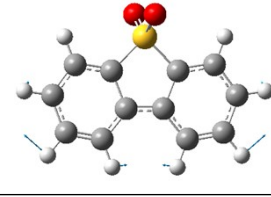
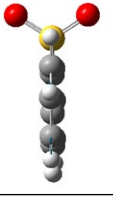
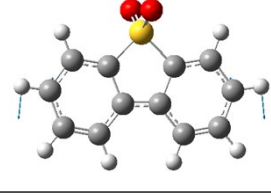
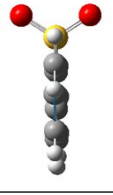
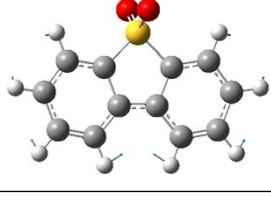
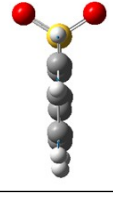
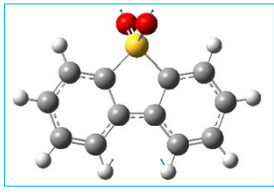
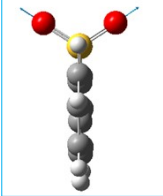
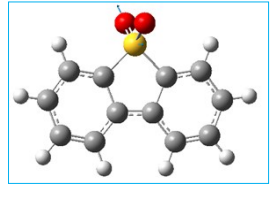
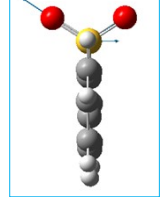
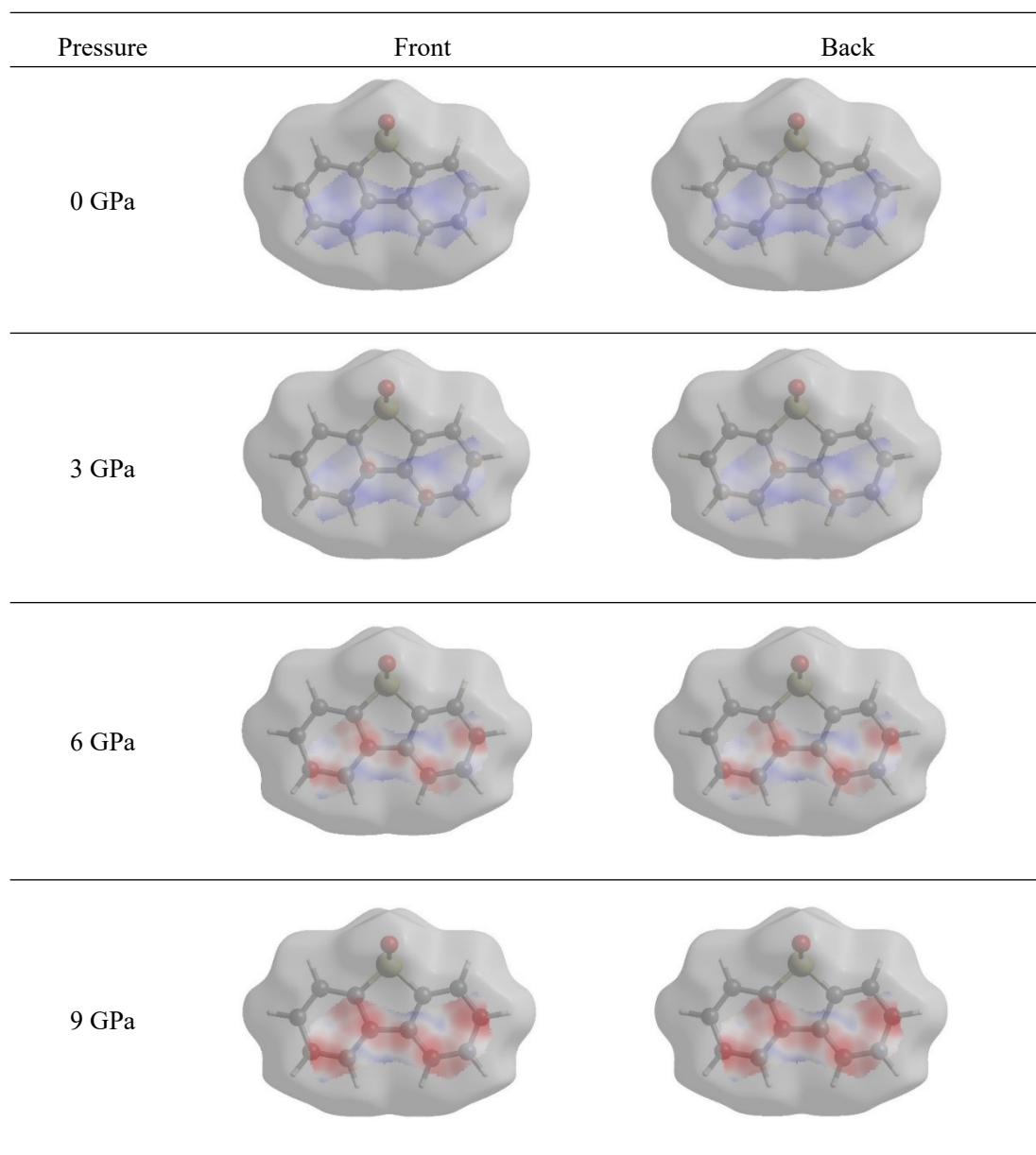
DBTS at excited state	356		
	1093		
	1152		
	1539		
	1605		
	1016 (S=O)		
	1167 (S=O)		

Table S4. The C \cdots C interactions on Hirshfeld surface at 0 GPa, 3 GPa, 6 GPa, 9 GPa.



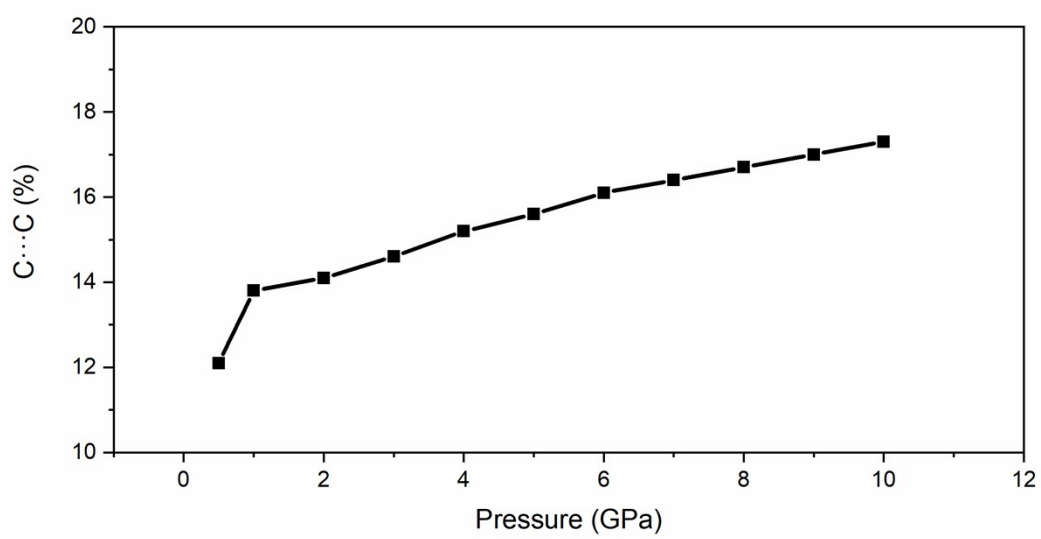


Figure S8. Contribution rate of C...C interactions to the Hirshfeld surface area versus pressure.

SIII Reference

- [1] Hohenberg, P.; Kohn, W. Inhomogeneous electron gas. *Phys. Rev.* 1964, 136, B864.
- [2] Clark, S. J.; Segall, M. D.; Pickard, C. J.; Hasnip, P. J.; Probert, M. I. J.; Refson, K.; Payne, M. C. First principles methods using CASTEP. *Z. Kristallogr. - Cryst. Mater.* 2005, 220, 567.
- [3] Perdew, J. P.; Burke, K.; Ernzerhof, M. Quantum theory group tulane university. *Phys. Rev. Lett.* 1996, 77, 3865.
- [4] Tkatchenko, A.; Scheffler, M. Accurate molecular van der Waals interactions from ground-state electron density and free-atom reference data. *Phys. Rev. Lett.* 2009, 102, 073005.
- [5] Spackman, P. R., Turner, M. J., McKinnon, J. J., Wolff, S. K., Grimwood, D. J., Jayatilaka, D. & Spackman, M. A. (2021). *J. Appl. Cryst.* 54, 3, 2021.
- [6] Spackman, M. A.; McKinnon, J. J. Hirshfeld surface analysis. *CrystEngComm* 2009, 11, 19.
- [7] Spackman, M. A.; McKinnon, J. J. Fingerprinting intermolecular interactions in molecular crystals. *CrystEngComm* 2002, 4, 378.
- [8] M. J. Frisch, G. W. Trucks, H. B. Schlegel, G. E. Scuseria, M. A. Robb, J. R. Cheeseman, G. Scalmani, V. Barone, B. Mennucci, G. A. Petersson, H. Nakatsuji, M. Caricato, X. Li, H. P. Hratchian, A. F. Izmaylov, J. Bloino, G. Zheng, J. L. Sonnenberg, M. Hada, M. Ehara, K. Toyota, R. Fukuda, J. Hasegawa, M. Ishida, T. Nakajima, Y. Honda, O. Kitao, H. Nakai, T. Vreven, J. A. Montgomery, Jr., J. E. Peralta, F. Ogliaro, M. Bearpark, J. J. Heyd, E. Brothers, K. N. Kudin, V. N. Staroverov, R. Kobayashi, J. Normand, K. Raghavachari, A. Rendell, J. C. Burant, S. S. Iyengar, J. Tomasi, M. Cossi, N. Rega, J. M. Millam, M. Klene, J. E. Knox, J. B. Cross, V. Bakken, C. Adamo, J. Jaramillo, R. Gomperts, R. E. Stratmann, O. Yazyev, A. J. Austin, R. Cammi, C. Pomelli, J. W. Ochterski, R. L. Martin, K. Morokuma, V. G. Zakrzewski, G. A. Voth, P. Salvador, J. J. Dannenberg, S. Dapprich, A. D. Daniels, Ö. Farkas, J. B. Foresman, J. V. Ortiz, J. Cioslowski and D. J. Fox, *Gaussian 09, Revision D.01*, Gaussian, Inc.: Wallingford CT, USA 2009.
- [9] J. R. Reimers, *J. Chem. Phys.* 2001, **115**, 9103.
- [10] Zheng, X. Y.; Peng, Q.; Zhu, L. Z.; Xie, Y. J.; Huang, X. H.; Shuai, Z. G., Unraveling the aggregation effect on amorphous phase AIE luminogens: a computational study. *Nanoscale* 2016, 8 (33), 15173-15180.
- [11] Zhang, T.; Shi, W.; Wang, D.; Zhuo, S.; Peng, Q.; Shuai, Z., Pressure-induced emission

enhancement in hexaphenylsilole: a computational study. *Journal of Materials Chemistry C* 2019, 7 (5), 1388-1398.

[12] Niu, Y.; Li, W.; Peng, Q.; Geng, H.; Yi, Y.; Wang, L.; Nan, G.; Wang, D.; Shuai, Z., MOlecular MAterials Property Prediction Package (MOMAP) 1.0: a software package for predicting the luminescent properties and mobility of organic functional materials. *Molecular Physics* 2018, 116 (7-8), 1078-1090.

[13] H. Yuan, K. Wang, K. Yang, B. Liu and B. Zou, *The Journal of Physical Chemistry Letters*, 2014, 5, 2968-2973.

[14] Y. Gu, H. Liu, R. Qiu, Z. Liu, C. Wang, T. Katsura, H. Zhang, M. Wu, M. Yao, H. Zheng, K. Li, Y. Wang, K. Wang, B. Yang, Y. Ma and B. Zou, *The Journal of Physical Chemistry Letters*, 2019, 10, 5557-5562.

[15] H. Yang, Z. Sun, C. Lv, M. Qile, K. Wang, H. Gao, B. Zou, Q. Song and Y. Zhang, *ChemPlusChem*, 2018, 83, 132-139.

[16] L. Wang, K. Wang, B. Zou, K. Ye, H. Zhang and Y. Wang, *Advanced Materials*, 2015, 27, 2918-2922.

[17] Y. Dong, J. Zhang, X. Tan, L. Wang, J. Chen, B. Li, L. Ye, B. Xu, B. Zou and W. Tian, *Journal of Materials Chemistry C*, 2013, 1, 7554-7559.

[18] Y. Dong, B. Xu, J. Zhang, X. Tan, L. Wang, J. Chen, H. Lv, S. Wen, B. Li, L. Ye, B. Zou and W. Tian, *Angewandte Chemie International Edition*, 2012, 51, 10782-10785.

[19] Y. Zhang, M. Qile, J. Sun, M. Xu, K. Wang, F. Cao, W. Li, Q. Song, B. Zou and C. Zhang, *Journal of Materials Chemistry C*, 2016, 4, 9954-9960.